molecules

MDPI

Article

The Suppression of Columnar π-Stacking in 3-Adamantyl-1-phenyl-1,4-dihydrobenzo[*e*][1,2,4]triazin-4-yl

Christos P. Constantinides [1,*], Andrey A. Berezin [1], Georgia A. Zissimou [1], Maria Manoli [1], Gregory M. Leitus [2] and Panayiotis A. Koutentis [1,*]

[1] Department of Chemistry, University of Cyprus, P. O. Box 20537, Nicosia 1678, Cyprus; berezin.andrey@ucy.ac.cy (A.A.B.); georgia_zissimou@hotmail.com (G.A.Z.); manoli.maria@ucy.ac.cy (M.M.)

[2] Department of Chemical Research Support, Weizmann Institute of Science, Rehovot 76100, Israel; gregory.leitus@weizmann.ac.il

* Correspondence: constantinides.christos@ucy.ac.cy (C.P.C.); koutenti@ucy.ac.cy (P.A.K.); Tel.: +357-22892783 (P.A.K.)

Academic Editor: Fawaz Aldabbagh
Received: 18 April 2016; Accepted: 10 May 2016; Published: 14 May 2016

Abstract: 3-Adamantyl-1-phenyl-1,4-dihydrobenzo[*e*][1,2,4]triazin-4-yl (**4**) crystallizes as chains of radicals where the spin bearing benzotriazinyl moieties are isolated from each other. Magnetic susceptibility studies in the 5–300 K temperature region indicate that radical **4** demonstrates typical paramagnetic behavior stemming from non-interacting $S = ½$ spins.

Keywords: 1,2,4-benzotriazinyls; hydrazyls; adamantyl; paramagnet; organic radicals; crystal packing

1. Introduction

1,4-Dihydrobenzo[*e*][1,2,4]triazin-4-yls a sub-class of the hydrazyl family of radicals has attracted considerable attention owing to their robust thermal, moisture and air stability. The first 1,2,4-benzotriazinyl radical was reported by Blatter in 1968 (Blatter radical **1**, Chart 1) [1], and, aside from electrochemical studies by Neugebauer [2–5], this stable radical remained relatively obscure. Nevertheless, the recent development of improved syntheses of 1,2,4-benzotriazinyls [6–10] have led to numerous new derivatives, some of which display a range of low dimensional magnetic properties [11–22], while others have been used as radical initiators in polymer chemistry [23–25], and as sensors of picric acid [18].

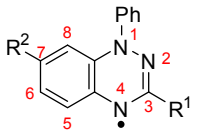

1 (R^1 = Ph, R^2 = H)
2 (R^1 = F_3C, R^2 = H)
3 (R^1 = Ph, R^2 = fur-2-yl)
4 (R^1 = 1-Ad, R^2 = H)

Chart 1. Structures of 1,2,4-benzotriazin-4-yls **1**–**4** and IUPAC numbering of the ring system.

Solid-state σ or π dimerization is suppressed in the majority of these radicals, nevertheless, for two derivatives radicals within the π-stacked columns associate leading to dimers with singlet ground states: (a) 1-phenyl-3-trifluoromethyl-1,4-dihydrobenzo[*e*]-[1,2,4]triazin-4-yl (**2**) demonstrates an abrupt fully reversible spin transition at 58(2) K between a diamagnetic low temperature phase and a paramagnetic high temperature phase [16] and (b) 7-(fur-2-yl)-1,3-diphenyl-1,4-dihydrobenzo[*e*][1,2,4]triazin-4-yl (**3**) has a singlet ground state below 100 K and a thermally accessible triplet state [13].

The extensive delocalization of the singly occupied molecular orbital (SOMO) orbital density over the benzo-fused hydrazonyl and the N1-Ph (Figure 1), indicates that positive orbital overlap and π-stacking, can be achieved in a variety of different association modes, and a number of different solid-state packing motifs have been reported [11–22]. In the majority of crystals structures reported to date, 1,2,4-benzotriazinyls π stack to form 1-D columns. The propensity of 1,2,4-benzotriazinyls to form columns could potentially be overcome by strategic introduction of bulky substituents in the periphery. To test this hypothesis we prepared a 1,2,4-benzotriazinyl substituted with an adamantyl group at C-3. Herein, we report the crystal structure and magnetic properties of the 3-adamantyl-1-phenyl-1,4-dihydrobenzo[*e*][1,2,4]triazin-4-yl (**4**).

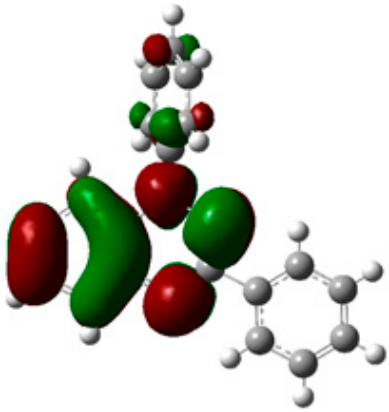

Figure 1. SOMO of Blatter radical **1** calculated at the UB3LYP/6-311+G(d,p).

2. Results and Discussion

2.1. Synthesis, Electrochemical and EPR Data

Radical **4** was previously prepared via a multistep route (Scheme 1) starting from the readily available 1-benzylidene-2-phenylhydrazine (**5**) [10]. Reaction of the benzylidene **5** with 1-fluoro-2-nitrobenzene and K_2CO_3 in DMSO at *ca.* 100 °C for 1 day gave 2-benzylidene-1-(2-nitrophenyl)-1-phenylhydrazine (**6**) which upon treatment with excess $NH_2OH\cdot HCl$ in pyridine and heating to *ca.* 80 °C for 1 day released 1-(2-nitrophenyl)-1-phenylhydrazine (**7**) in 80% yield. Acetylation and subsequent mild reduction of the nitro group followed by an acid-mediated cyclodehydration gave the fused triazine which upon alkali treatment afforded the desired adamantly-substituted radical **4**.

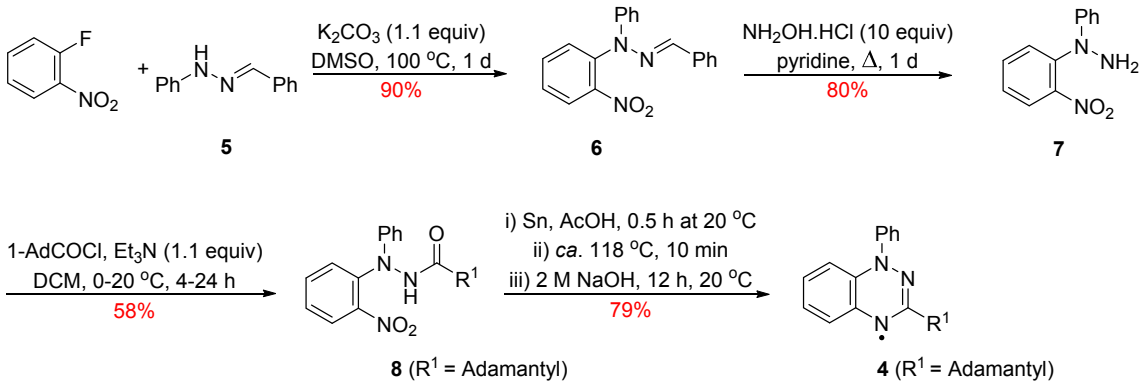

Scheme 1. Synthesis of the 3-adamantyl-1,2,4-benzotriazinyl **4**.

The redox behavior of radical **4** is typical of 1,2,4-benzotriazinyls exhibiting two fully reversible waves corresponding to the −1/0 and 0/+1 processes (Figure 2, left) [11–22]. Worthy of note is that the

oxidation potential of $E_{1/2}{}^{0/+1}$ = 0.08 V *vs* Fc/Fc$^+$ couple makes radical **4** the best 1,2,4-benzotriazinyl donor reported to date. The solution EPR spectrum of radical **4** (Figure 2, right) exhibits the typical 1,2,4-benzotriazinyl seven-line multiplets consistent with coupling of the unpaired electron with the three similar but slightly nonequivalent ^{14}N nuclei. The hyperfine coupling constants (hfcc), determined by the simulation of the EPR spectrum, are $a_{N(1)}$ = 7.51, $a_{N(2)}$ = 4.94 and $a_{N(4)}$ = 5.13 G with g = 2.0040.

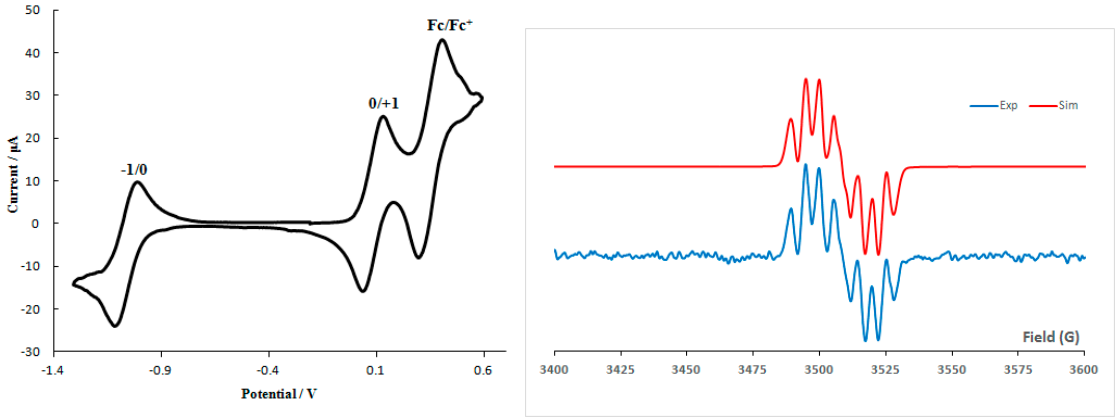

Figure 2. Cyclic voltammetry (**left**) and solution EPR spectrum (**right**) of radical **4**.

2.2. X-ray Studies

Suitable single crystals of radical **4** for X-ray diffraction studies were obtained by slow cooling of a concentrated *c*-hexane solution. Radical **4** adopted the orthorhombic space group *Pna*2$_1$ with two molecules in the asymmetric unit. These two molecules are oriented in a dihedral angle of 56.9° with respect to each other (Figure 3). The intramolecular geometry of radical **4** is typical of other 1,2,4-benzotriazinyls [11–22].

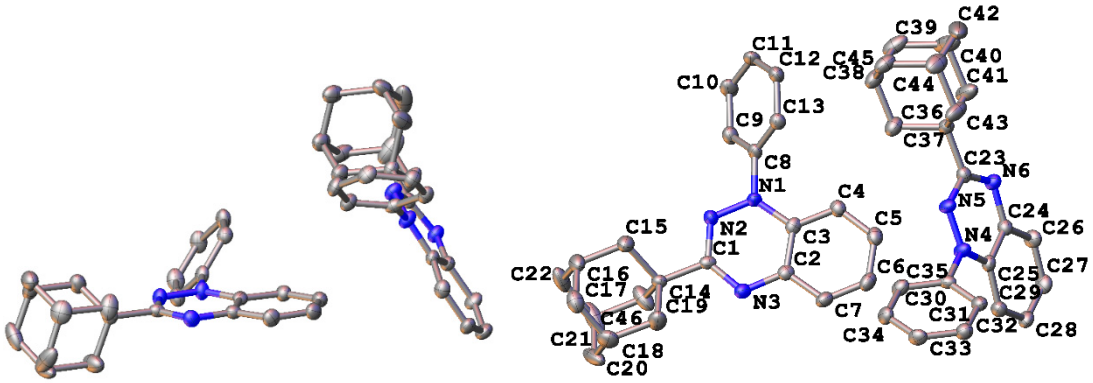

Figure 3. Asymmetric unit (**left**) and crystallographic atom numbering for 3-adamantyl-1,2,4-benzotriazinyl **4** (**right**). Hydrogen atoms omitted for clarity.

Each molecule in the asymmetric unit forms a linear chain of radicals at regular distances. Radicals in the chain running parallel to *c*-axis (Figure 4, top) have two close contacts, one between neighboring adamantyls [$d_{C46\ldots C19}$ = 4.297(5)°] and one between adamantyl and benzotriazinyl [$d_{C20\ldots C1}$ = 3.828(5)°]. Radicals within this chain are related by a 2-fold screw axis with direction (0, 0, 1) at 0,0,z and screw component (0, 0, ½). Radicals in the second chain running parallel to *a*-axis (Figure 4, bottom) are connected via a weak hydrogen contact between neighboring benzotriazinyls [$d_{N6\ldots C34}$ = 3.585(4)°]. This contact may propagate an antiferromagnetic interaction between the positive spin density on N6 and the negative spin density on C34. Carbon C34 has minimal orbital

density in the SOMO, however, through spin polarization, it possesses significant negative spin density. The radical chains are related by two glide planes, one perpendicular to (0, 1, 0) with glide component (½, 0, 0) and one perpendicular to (1, 0, 0) with glide component (0, ½, ½). No formation of columns by π-stacked radicals was observed. The spin bearing benzotriazinyl moieties do not interact with each other. The related 3-(*tert*-butyl)-1-phenyl-1,4-dihydro-1,2,4-benzotriazin-4-yl was shown to crystallize in 1-D columns without π-π interactions between the benzotriazinyl moieties [5,20]. This radical demonstrated typical paramagnetic behavior as it followed the Curie-Weiss law with $\theta = -0.3$ K [5].

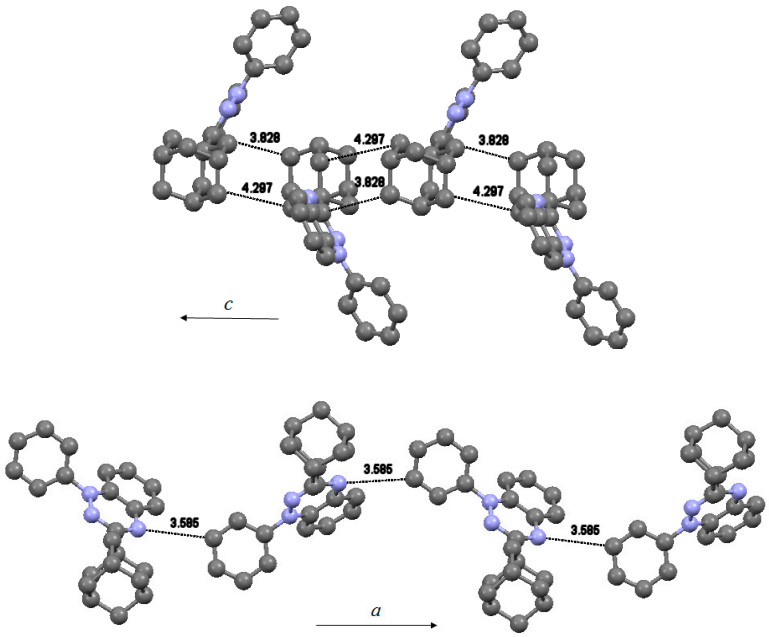

Figure 4. Solid-state packing of radical **4** demonstrating the formation of chains along *c*-axis (**top**) and along *a*-axis (**bottom**).

2.3. Magnetic Susceptibility Studies

Variable-temperature magnetic-susceptibility measurements on radical **4** were obtained using a SQUID magnetometer in the temperature region 5–300 K in an applied field of 0.4 T. Data were collected in both warming and cooling modes with no significant differences in sample susceptibility. The temperature dependence of χT is shown in Figure 5.

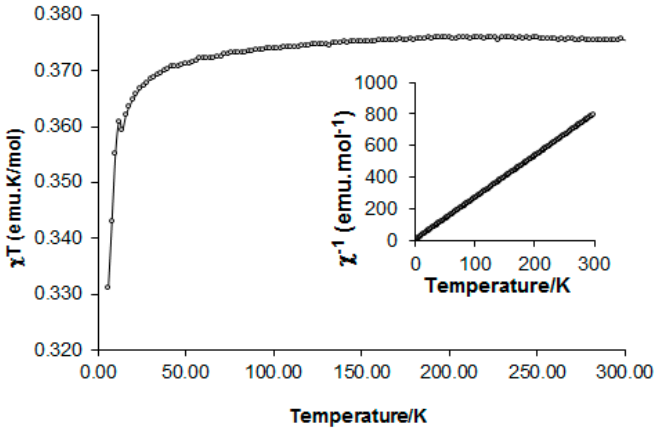

Figure 5. Temperature dependence of χT upon heating from 5 to 300 K. Inset: Curie-Weiss behavior, $C = 0.377$ emu K·mol^{-1} and $\theta = -0.61$ K.

The inverse of molar susceptibility ($1/\chi$) followed the Curie-Weiss law (Figure 5, inset) with $C = 0.377$ emu K·mol^{-1} and $\theta = -0.61$ K. On cooling from 300 K down to *ca.* 50 K, χT remained stable with a value of 0.375 emu K·mol^{-1} expected for an $S = ½$ paramagnet. Below 50 K, χT gradually decreased as antiferromagnetic interactions along the a-axis chain (weak hydrogen $d_{N6 \ldots C34}$ contacts) became dominant.

3. Experimental Sections

Synthetic procedure: The synthesis of radical **4** was published previously [10].

Instrumental analyses: Cyclic voltammetry (CV) measurements were performed on a Princeton Applied Research Potentiostat/Galvanostat 263A apparatus (Oak Ridge, TN, USA). The concentration of the benzotriazinyl radical **4** used was 1 mM in CH_2Cl_2. A 0.1 M CH_2Cl_2 solution of tetra-butylammonium tetrafluoroborate (n-Bu_4BF_4) was used as electrolyte. The electrolyte was dried for four days in the vacuum oven at 100 °C prior to the use. The reference electrode was Ag/AgCl and the scan rate was 50 mV/s. Ferrocene was used as an internal reference; the $E_{1/2}$(ox) of ferrocene in this system was 0.352 V [26]. EPR spectra were recorded on a Bruker EMXplus X-band EPR spectrometer (Bruker, Billerica, MA, USA) at room temperature in dilute solution of CH_2Cl_2. For the EPR spectrum, the microwave power was in the region 5–70 mW with modulation frequencies of 50 or 100 kHz and modulation amplitudes of 0.5–1.0 G_{pp}. Simulations of the solution spectrum was made using Winsim software [27]. X-ray data of **4** (CCDC 1474192) [28] were collected on an Oxford-Diffraction Supernova diffractometer, equipped with a CCD area detector utilizing Mo-Kα radiation ($\lambda = 0.71073$ Å). A suitable crystal was attached to glass fibers using paratone-N oil and transferred to a goniostat where they were cooled for data collection. Unit cell dimensions were determined and refined by using 4562 ($3.85 \leqslant \theta \leqslant 27.68^{\circ}$) reflections. Empirical absorption corrections (multi-scan based on symmetry-related measurements) were applied using CrysAlis RED software [29]. The structures were solved by direct method and refined on F^2 using full-matrix least squares using SHELXL97 [30,31]. Software packages used: CrysAlis CCD [29] for data collection, CrysAlis RED [29] for cell refinement and data reduction, WINGX for geometric calculations [32] and Mercury 3.1 (CCDC, Cambridge, UK) [33]. The non-H atoms were treated anisotropically. The hydrogen atoms were placed in calculated, ideal positions and refined as riding on their respective carbon atoms. Magnetic properties were studied by using a Quantum Design SQUID $MPMS_2$ field-shielded magnetometer (Quantum Design Inc., San Diego, CA, USA). The DC (direct current) magnetic moment was measured for 43 mg sample of radical **4**, placed in gelatin capsules held by polyethylene straw. The magnetic susceptibilities were measured in the temperature range of 5–300 K in an applied field of 0.4 T. Data were collected in both warming and cooling modes with no significant differences in sample susceptibility.

Crystal refinement data (**4**): $C_{23}H_{24}N_3$, $M = 342.45$, Orthorhombic, space group *Pna21*, $a = 18.5886(10)$ Å, $b = 19.3115(9)$ Å, $c = 9.9148(6)$ Å, $\alpha = 90^{\circ}$, $\beta = 90^{\circ}$, $\gamma = 90^{\circ}$, $V = 35.59(2)$ Å^3, $Z = 8$, T = 100(2) K, $\rho_{calcd} = 1.278$ g·cm^{-3}, $2\theta_{max} = 25$. Refinement of 470 parameters on 5357 independent reflections out of 12978 measured reflections ($R_{int} = 0.0438$) led to $R_1 = 0.04761$ [$I > 2\sigma(I)$], $wR_2 = 0.1154$ (all data), and $S = 1.050$ with the largest difference peak and hole of 0.227 and -0.176×10^{-3}, respectively.

4. Conclusions

Introduction of the bulky substituent adamantyl to the C-3 position of the 1,2,4-benzotriazinyl framework successfully inhibited the formation of π-stacked radical columns, but instead of promoting higher dimensional frameworks, only isolated radicals were obtained. This led to non-interacting $S = ½$ spins and a typical paramagnetic behavior. Our results indicate that there is a fine balance to be reached between steric perturbation and π-stacking interactions if materials with interesting magnetic and transport properties are to be developed.

Acknowledgments: The authors thank the University of Cyprus (medium-size grants), the Cyprus Research Promotion Foundation (grants no. ΥΓΕΙΑ/ΒΙΟΣ/0308(ΒΙΕ)/13, ΝΕΚΥΠ/0308/02 and ΑΝΑΒΑΘΜΙΣΗ/0308/32

and the following organizations in Cyprus for generous donations of chemicals and glassware: the State General Laboratory, the Agricultural Research Institute, the Ministry of Agriculture, MedoChemie Ltd. and Biotronics Ltd. Furthermore, we thank the A. G. Leventis Foundation for helping to establish the NMR facility in the University of Cyprus.

Author Contributions: Christos P. Constantinides and Panayiotis A. Koutentis have contributed to the conception, drafting and critical revision of the submitted manuscript. Andrey A. Berezin and Georgia A. Zissimou have contributed to the synthesis of the radical and collection of data. Maria Manoli has acquired the X-ray diffraction data and solved the structure. Gregory M. Leitus has acquired the magnetometry data.

Conflicts of Interest: The authors declare no conflict of interest.

References and Notes

1. Blatter, H.M.; Lukaszewshki, H. A new stable free radical. *Tetrahedron Lett.* **1968**, *9*, 2701–2705. [CrossRef]
2. Neugebauer, F.A.; Umminger, I. Über 1,4-Dihydro-1,2,4-benzotriazinyl-Radikale. *Chem. Ber.* **1980**, *113*, 1205–1225. [CrossRef]
3. Neugebauer, F.A.; Umminger, I. 1,4-Dihydro-1,2,4-benzotriazin-Radikalkationen. *Chem. Ber.* **1981**, *114*, 2423–2430. [CrossRef]
4. Neugebauer, F.A.; Rimmler, G. ENDOR and Triple Resonance Studies of 1,4-Dihydro-1,2,4-benzotriazinyl Radicals and 1,4-Dihydro-1,2,4-benzotriazine Radical Cations. *Magn. Reson. Chem.* **1988**, *26*, 595–600. [CrossRef]
5. Mukai, K.; Inoue, K.; Achiwa, N.; Jamali, J.B.; Krieger, C.; Neugebauer, F.A. Magnetic properties of 1,4-dihydro-1,2,4-benzotriazin-4-yl radicals. *Chem. Phys. Lett.* **1994**, *224*, 569–575. [CrossRef]
6. Koutentis, P.A.; Lo Re, D. Catalytic Oxidation of *N*-Phenylamidrazones to 1,3-Diphenyl-1,4-dihydro-1,2,4-benzotriazin-4-yls: An Improved Synthesis of Blatter's Radical. *Synthesis* **2010**, 2075–2079. [CrossRef]
7. Constantinides, C.P.; Koutentis, P.A.; Loizou, G. Synthesis of 7-aryl/heteraryl-1,3-diphenyl-1,2,4-benzotriazinyls via palladium catalyzed Stille and Suzuki-Miyaura reactions. *Org. Biomol. Chem.* **2011**, *9*, 3122–3125. [CrossRef] [PubMed]
8. Berezin, A.A.; Constantinides, C.P.; Drouza, C.; Manoli, M.; Koutentis, P.A. From Blatter Radical to 7-Substituted 1,3-Diphenyl-1,4-dihydrothiazolo[5′,4′:4,5]benzo[1,2-*e*][1,2,4]triazin-4-yls: Toward Multifunctional Materials. *Org. Lett.* **2012**, *14*, 5586–5589. [CrossRef] [PubMed]
9. Berezin, A.A.; Constantinides, C.P.; Mirallai, S.I.; Manoli, M.; Cao, L.L.; Rawson, J.M.; Koutentis, P.A. Synthesis and properties of imidazolo-fused benzotriazinyl radicals. *Org. Biomol. Chem.* **2013**, *11*, 6780–6795. [CrossRef] [PubMed]
10. Berezin, A.A.; Zissimou, G.A.; Constantinides, C.P.; Beldjoudi, Y.; Rawson, J.M.; Koutentis, P.A. Route to Benzo- and Pyrido-Fused 1,2,4-Triazinyl Radicals via *N*′-(Het)aryl-*N*′-[2-nitro(het)aryl]hydrazides. *J. Org. Chem.* **2014**, *79*, 314–327. [CrossRef] [PubMed]
11. Constantinides, C.P.; Koutentis, P.A.; Krassos, H.; Rawson, J.M.; Tasiopoulos, A.J. Characterization and Magnetic Properties of a "Super Stable" Radical 1,3-Diphenyl-7-trifluoromethyl-1,4-dihydro-1,2,4-benzotriazin-4-yl. *J. Org. Chem.* **2011**, *76*, 2798–2806. [CrossRef] [PubMed]
12. Constantinides, C.P.; Koutentis, P.A.; Rawson, J.M. Antiferromagnetic Interactions in 1D Heisenberg Linear Chains of 7-(4-Fluorophenyl) and 7-Phenyl-Substituted 1,3-Diphenyl-1,4-dihydro-1,2,4-benzotriazin-4-yl Radicals. *Chem. Eur. J.* **2012**, *18*, 15433–15438. [CrossRef] [PubMed]
13. Constantinides, C.P.; Carter, E.; Murphy, D.M.; Manoli, M.; Leitus, G.M.; Bendikov, M.; Rawson, J.M.; Koutentis, P.A. Spin-triplet excitons in 1,3-diphenyl-7-(fur-2-yl)-1,4-dihydro-1,2,4-benzotriazin-4-yl. *Chem. Commun.* **2013**, *49*, 8662–8664. [CrossRef] [PubMed]
14. Constantinides, C.P.; Berezin, A.A.; Manoli, M.; Leitus, G.M.; Bendikov, M.; Rawson, J.M.; Koutentis, P.A. Effective exchange coupling in alternating-chains of a π-extended 1,2,4-benzotriazin-4-yl. *New J. Chem.* **2014**, *38*, 949–954. [CrossRef]
15. Constantinides, C.P.; Berezin, A.A.; Manoli, M.; Leitus, G.M.; Zissimou, G.Z.; Bendikov, M.; Rawson, J.M.; Koutentis, P.A. Structural, Magnetic, and Computational Correlations of Some Imidazolo-Fused 1,2,4-Benzotriazinyl Radicals. *Chem. Eur. J.* **2014**, *20*, 5388–5396. [CrossRef] [PubMed]

16. Constantinides, C.P.; Berezin, A.A.; Zissimou, G.Z.; Manoli, M.; Leitus, G.M.; Bendikov, M.; Probert, M.R.; Rawson, J.M.; Koutentis, P.A. A Magnetostructural Investigation of an Abrupt Spin Transition for 1-Phenyl-3-trifluoromethyl-1,4-dihydrobenzo[*e*][1,2,4]triazin-4-yl. *J. Am. Chem. Soc.* **2014**, *136*, 11906–11909. [CrossRef] [PubMed]
17. Yan, B.; Cramen, J.; McDonald, R.; Frank, N.L. Ferromagnetic spin-delocalized electron donors for multifunctional materials: π-Conjugated benzotriazinyl radicals. *Chem. Comm.* **2011**, *47*, 3201–3203. [CrossRef] [PubMed]
18. Zheng, Y.; Miao, M.-S.; Kemei, M.C.; Seshadri, R.; Wudl, F. The Pyreno-Triazinyl Radical–Magnetic and Sensor Properties. *Isr. J. Chem.* **2014**, *54*, 774–778. [CrossRef]
19. Takahashi, Y.; Miura, Y.; Yoshioka, N. Introduction of Three Aryl Groups to Benzotriazinyl Radical by Suzuki-Miyaura Cross-coupling Reaction. *Chem. Lett.* **2014**, *43*, 1236–1238. [CrossRef]
20. Takahashi, Y.; Miura, Y.; Yoshioka, N. Synthesis and properties of the 3-*tert*-butyl-7-trifluoromethyl-1,4-dihydro-1-phenyl-1,2,4-benzotriazin-4-yl radical. *New J. Chem.* **2015**, *39*, 4783–4789. [CrossRef]
21. Miura, Y.; Yoshioka, N. π-Stacked structure of thiadiazolo-fused benzotriazinyl radical: Crystal structure and magnetic properties. *Chem. Phys. Lett.* **2015**, *626*, 11–14. [CrossRef]
22. Fumanal, M.; Vela, S.; Novoa, J.J.; Ribas-Arino, J. Towards the tailored design of benzotriazinyl-based organic radicals displaying a spin transition. *Chem. Commun.* **2015**, *51*, 15776–15779. [CrossRef] [PubMed]
23. Demetriou, M.; Berezin, A.A.; Koutentis, P.A.; Krasia-Christoforou, T. Benzotriazinyl-mediated controlled radical polymerization of styrene. *Polym. Int.* **2014**, *63*, 674–679. [CrossRef]
24. Areephong, J.; Treat, N.; Kramer, J.W.; Christianson, M.D.; Hawker, C.J.; Collins, H.A. Triazine Mediated Living Radical Controlled Polymerization. WO 2015/061189 A1, 30 April 2015.
25. Areephong, J.; Mattson, K.M.; Treat, N.J.; Poelma, S.O.; Kramer, J.W.; Sprafke, H.A.; Latimer, A.A.; Read de Alaniz, J.; Hawker, C.J. Triazine-Mediated Controlled Radical Polymerization: New Unimolecular Initiators. *Polym. Chem.* **2016**, *7*, 370–374. [CrossRef]
26. Dietrich, M.; Heinze, J. On the Determination of Redox Potentials of Highly Reactive Aromatic Mono- and Multications. *J. Am. Chem. Soc.* **1990**, *112*, 5142–5145. [CrossRef]
27. Duling, D.R. Simulation of Multiple Isotropic Spin Trap EPR Spectra. *J. Magn. Reson. Ser. B* **1994**, *104*, 105–110. [CrossRef]
28. CCDC 1474192 contains the supplementary crystallographic data for this paper. These data can be obtained free of charge via http://www.ccdc.cam.ac.uk/conts/retrieving.html (or from the CCDC, 12 Union Road, Cambridge CB2 1EZ, UK; Fax: +44 1223 336033; E-mail: deposit@ccdc.cam.ac.uk.
29. *CrysAlis CCD and CrysAlis RED, version 1.171.32.15*; Oxford Diffraction Ltd: Abingdon, Oxford, UK, 2008.
30. Sheldrick, G.M. *SHELXL 97-A Program for the Refinement of Crystal Structure*; University of Göttingen: Göttingen, Germany, 1997.
31. Sheldrick, G.M. A short history of *SHELX*. *Acta. Cryst.* **2008**, *A64*, 112–122. [CrossRef] [PubMed]
32. Farrugia, L.J. *WinGX* suite for small-molecule single-crystal crystallography. *J. Appl. Crystallogr.* **1999**, *32*, 837–838.
33. Macrae, C.F.; Edgington, P.R.; McCabe, P.; Pidcock, E.; Shields, G.P.; Taylor, R.; Towler, M.; van de Streek, J. Mercury: Visualization and analysis of crystal structures. *J. Appl. Cryst.* **2006**, *39*, 453–457. [CrossRef]

Sample Availability: Sample of the radical is available from the authors.